20

Amplitude Phase Shift Keying Constellation Design and its Applications to Satellite Digital Video Broadcasting

Konstantinos P. Liolis[1], Riccardo De Gaudenzi[2], Nader Alagha[3], Alfonso Martinez[4], and Albert Guillén i Fàbregas[5]

[1]*Space Hellas S.A., R&D and Applications Division, 312 Messogion Ave., 153 41, Athens, Greece*

[2,3]*European Space Agency (ESA/ESTEC), Keplerlaan 1, P.O. Box 299, 2200 AG, Noordwijk, The Netherlands*

[4]*Centrum Wiskunde & Informatica (CWI), Science Park 123, 1098 XG, Amsterdam, The Netherlands*

[5]*University of Cambridge, Department of Engineering, Trumpington Street, CB2 1PZ, Cambridge, UK*

1. Introduction

Satellite communications are providing a key role in the worldwide digital information networks. Among other applications, satellite communications provide the platform for Direct-to-Home (DTH) digital TV broadcasting as well as interactive and subscription TV services, mobile services to ships, aircraft and land-based users, and data distribution within business networks. Satellite networks are essential part of the Internet backbone enabling both broadband and narrowband Internet access services from remote and rural areas where the satellite access provide a unique way to complement the terrestrial telecommunication infrastructure. Moreover, satellite networks will play a crucial role in the framework of the Future Internet [Future Internet, 2009].

Recent trends in satellite communications show an increasing demand to replace or complement conventional modulation schemes, such as Quaternary Phase Shift Keying (QPSK), with higher-order *M*-ary modulation schemes. Some contributing factors that enable such trends are as follows [Alberty *et al.*, 2007; Benedetto *et al.*, 2005; Rinaldo & De Gaudenzi, 2004a; Rinaldo & De Gaudenzi, 2004b]:

- The usage of higher frequency bands (e.g., from X, Ku, up to Ka and Q).
- The exploitation of capacity boosting techniques, such as Adaptive Coding and Modulation (ACM) which are enabling the commercial exploitation of high frequency bands.
- The higher frequency reuse achievable with multibeam satellite antennas.
- The increasing satellite Effective Isotropic Radiated Power (EIRP) at RF as well as satellite antenna Gain over noise Temperature (G/T) becoming available thanks to payload and antenna technology improvements.

Source: Digital Video, Book edited by: Floriano De Rango,
ISBN 978-953-7619-70-1, pp. 500, February 2010, INTECH, Croatia, downloaded from SCIYO.COM

- The availability of wideband satellite transponders as well as the deep submicron Application Specific Integrated Circuit (ASIC) technology allowing the support of high data rate modems (i.e. single carrier transponder operation with hundreds of Mbaud).

Nevertheless, these technical enhancements require the exploitation of highly efficient coding techniques associated with power- and spectrally- efficient modulation schemes designed to operate over the satellite channel environment. Higher-order *M*-ary modulation schemes can provide greater spectral efficiency and thus the high data rate required for either digital multimedia applications or other applications such as point-to-point high data-rate backbone connectivity and future Earth observation missions requiring downlink data rates exceeding 1 Gbps. In this regard, Amplitude Phase Shift Keying (APSK) represents an attractive modulation scheme for digital transmission over nonlinear satellite channels due to its power and spectral efficiency combined with its inherent robustness against nonlinear distortion. The concept of circular APSK modulation and its suitability for nonlinear channels was already proposed in 1970's [Thomas *et al.*, 1974] but, at that time, it was concluded that APSK performs worse than PSK schemes for single carrier operation over nonlinear channel. However, based on the recent pioneering work of some of the authors reported in [De Gaudenzi *et al.*, 2006a; De Gaudenzi *et al.*, 2006b], this conclusion was reverted and thus APSK has become nowadays a state-of-the-art modulation scheme for advanced satellite communications. As an illustration, APSK has been recently adopted in the following commercial standards related to satellite digital video broadcasting:

- DVB-S2 (Digital Video Broadcasting via Satellite – 2nd generation) [DVB-S2, 2005]: It is the ETSI standard for the forward link of satellite digital video broadcasting systems mainly operating at Ku (12/14 GHz) and Ka (20/30 GHz) frequency bands and targeting mainly fixed users but also mobile collective platforms, such as airplanes, ships and trains.
- DVB-SH (Digital Video Broadcasting via Satellite to Handheld devices) [DVB-SH, 2007]: It is the ETSI standard for the forward link of hybrid satellite/terrestrial digital video broadcasting systems operating at L (1/2 GHz) and S (2/4 GHz) frequency bands targeting mainly mobile users, such as handheld devices and vehicles.
- IPoS (Internet Protocol over Satellite) [IPoS, 2006]: It is the ETSI standard for broadband interactive satellite networks that has adopted DVB-S2 with ACM for its forward link. This standard has been proposed and adopted by the biggest interactive satellite networks manufacturer [Hughes, 2009].
- GMR-1 3G (Geostationary Mobile Radio – 3rd Generation) [GMR-1 3G, 2008]: It is a new ETSI standard for Mobile Satellite Systems (MSS) whose Release 3 has evolved to a 3G satellite-based packet service equivalent to 3GPP terrestrial mobile standard for the support of voice, data and video applications.
- ABS-S (Advanced Broadcasting System via Satellite) [Yuhai Shi *et al.*, 2008]: It is the Chinese standard for the forward link of satellite digital video broadcasting systems operating at Ku frequency band and targeting mainly fixed users and DTH applications.

The abovementioned standards have adopted the 16- and 32-APSK modulation schemes, whose constellation design has been described in [De Gaudenzi *et al.*, 2006a; De Gaudenzi *et al.*, 2006b]. These modulation schemes are mainly considered for professional applications where the satellite terminal sizing (i.e., antenna size and High Power Amplified (HPA)) allows for adequate Signal-to-Noise Ratio (SNR) at the receiver. However, APSK modulations can also be used for interactive consumer applications in case of multibeam

satellites or digital video broadcasting when higher spectral efficiency is needed. More recently, there has also been an increasing commercial interest to go beyond the standardized 16- and 32-APSK modes especially in professional applications such as Digital Satellite News Gathering (DSNG) where even higher requirements in terms of available SNR apply. Thus, design optimization for 64-APSK modulation has been addressed in [Liolis & Alagha, 2008; Benedetto *et al*., 2005]. The reported results particularly in [Benedetto *et al*., 2005] were obtained as part of the ESA project "Modem for High Order Modulation Schemes" whose technical baseline has been recently proposed as potential standard for space telemetry related applications [CCSDS, 2007]. The APSK constellation design approaches considered in [De Gaudenzi *et al*., 2006a; De Gaudenzi *et al*., 2006b; Liolis & Alagha, 2008] follow two main optimization criteria: (i) maximization of the minimum Euclidean distance, and (ii) maximization of the channel mutual information. Unlike the former optimization criterion which refers to the high SNR asymptotic case, the latter provides an optimum *M*-APSK constellation for each SNR operating point. The design optimization analysis and results obtained for 16-, 32- and 64-APSK modulation schemes based on the mutual information maximization criterion are presented in detail in this chapter assuming error correction coding and taking into account both cases of equiprobable and non-equiprobable constellations.

Although these higher-order *M*-ary APSK modulation schemes have been specifically designed for operating over nonlinear satellite channels, they still show signal envelope fluctuations and are particularly sensitive to the characteristics of the satellite transponders which introduce channel nonlinearities. Examples of performance analysis of APSK signal transmission over nonlinear satellite channel and error rate bounds are reported in [Sung *et al*., 2009]. As has been shown in [Casini *et al*., 2004; De Gaudenzi *et al*., 2006b] and in references therein, the power efficiency of APSK modulation schemes can be improved by applying pre-distortion on the transmit data, avoiding large input and output back-off values on the satellite transponder (or in the ground terminal HPA). Pre-distortion means intentionally modifying the location of the data symbols on the complex plane with respect to their nominal position. Such a technique only calls for a modification of the transmitted constellation points and this is particularly straightforward and effective for circular constellations such as APSK. Different pre-distortion schemes have been investigated in the literature, based on either "instantaneous" evaluation of the constellation centroids distortion at the receiver (adaptive *static* pre-distortion) [De Gaudenzi *et al*., 2006b] or consideration of a certain amount of "memory" in the combined phenomenon of nonlinear distortion plus matched filtering at the receiver (adaptive *dynamic* pre-distortion) [Karam & Sari, 1991]. Despite the hardware complexity impact, commercial satellite modems have already adopted relevant dynamic pre-distortion techniques for standardized 16- and 32-APSK modes [Newtec, 2009], which are presented in this chapter.

The rest of this chapter is organized as follows. Section 2 describes the system model and the main effects of the nonlinear amplifier. Section 3 provides a formal description of APSK signal sets, describes the APSK constellation design optimization criterion of maximum mutual information and discusses some of the properties of the optimized constellations for the equiprobable and non-equiprobable cases. In Section 4, practical static and dynamic nonlinearity distortion pre-compensation techniques of commercial interest are described. Useful numerical results illustrating the system design tradeoffs for APSK constellations over typical satellite channels along with some practical design guidelines for system engineers

with regard to the application of APSK constellations for satellite digital video broadcasting are also provided along Sections 3-4. Finally, concluding remarks are drawn in Section 5.

2. System model

We consider a communication system composed of a digital modulator, a Square-Root Raised Cosine (SRRC) band-limiting filter and a nonlinear HPA with typical Travelling Wave Tube Amplifier (TWTA) characteristic for a satellite operating in Ku or Ka band. This model is representative of a satellite bent-pipe transponder with uplink noise negligible compared to the downlink. Due to the tight signal band-limiting, the impact of the satellite input and output analog filters is assumed negligible. In any case, satellite filters' linear distortions can be easily compensated through simple demodulator digital equalizers. The baseband equivalent of the transmitted signal at time t, $s_T(t)$, is given by

$$s_T(t) = \sqrt{P}\sum_{k=0}^{L-1} x(k)\, p_T(t - kT_s) \tag{1}$$

where P is the signal power, $x(k)$ is the k-th transmitted symbol drawn from a complex-valued APSK signal constellation $\mathfrak{X}$ with cardinality $|\mathfrak{X}| = M$, $p_T(t)$ is the SRRC transmission filter impulse response and T_s is the transmitted symbol duration (in seconds). Without loss of generality, we consider transmission of frames with L symbols. The coded modulation spectral efficiency R is the number of information bits normalised by the modulator baud rate. Equivalently, $R = r\log_2 M$, where r is the coding rate.
The signal $s_T(t)$ passes through the HPA which is operated close to the saturation point. In this region, the HPA shows nonlinear characteristics that induce phase and amplitude distortions to the transmitted signal. The HPA is modelled by a memoryless nonlinearity, with an output signal $s_A(t)$ at time t given by

$$s_A(t) = F(|s_T(t)|)\exp\left[j\left(\phi(s_T(t)) + \Phi(|s_T(t)|)\right)\right] \tag{2}$$

where we have implicitly defined $F(A)$ and $\Phi(A)$ as the Amplitude-to-Amplitude Modulation (AM/AM) and Amplitude-to-Phase Modulation (AM/PM) characteristics of the HPA amplifier for a signal with instantaneous amplitude A. As an illustration, the AM/AM and AM/PM characteristics of a typical Ka band TWTA is depicted in Fig. 1. The signal amplitude is the instantaneous complex envelope so that the baseband equivalent signal is denoted as $s_T(t) = |s_T(t)|\exp[j\varphi(s_T(t))]$.

2.1 Linear AWGN channel model

In this case, we assume an (ideal) signal modulating a train of rectangular pulses, which do not create Inter-Symbol Interference (ISI) when passed through the HPA operated in the nonlinear region [De Gaudenzi *et al.*, 2006a]. Under these conditions, the channel reduces to an Additive White Gaussian Noise (AWGN), where the modulation symbols are distorted following (2). Let x_A denote the distorted symbol corresponding to $x = |x|\exp[j\varphi(x)] \in \mathfrak{X}$, i.e.,

$$x_A = F(|x|)\exp\left[j\left(\phi(x) + \Phi(|x|)\right)\right] \tag{3}$$

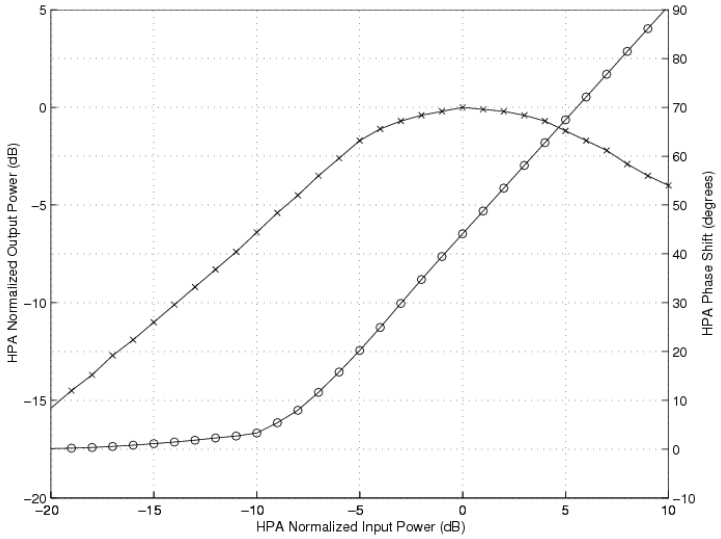

Fig. 1. AM/AM (crosses '+') and AM/PM (circles '○') characteristics of the reference Ka band TWTA.

After matched filtering and sampling at time kT_s, the discrete-time received signal at time k is then given by

$$y(k) = \sqrt{E_s}\, x_A(k) + n(k),\ k = 0,1,...,L-1 \tag{4}$$

where E_s is the symbol energy given by $E_s=PT_s$, $x_A(k)$ is the symbol at the k-th time instant as defined in (3) and $n(k) \sim N_{\mathbb{C}}(0, N_0)$ is the corresponding noise sample.

2.2 Non-Linear channel model

In this case, we introduce the parameter $E_b/N_0|_{\text{sat}}$ defined as the ratio between the transmitted energy per bit E_b when the amplifier is driven at saturation by a continuous wave carrier and the noise power spectral density N_0 at the demodulator input. Note that the subscript "sat" refers to the HPA saturation. The SNR at the demodulator input $E_b/N_0|_{\text{inp}}$ is reduced by the Output Back-Off (OBO, in dB) with respect to the value in a system operating with a single constant-envelope signal at amplifier saturation (in dB):

$$\left.\frac{E_b}{N_0}\right|_{sat}(IBO) = \left.\frac{E_b}{N_0}\right|_{inp}(IBO) + OBO(IBO) \tag{5}$$

where IBO is the satellite transponder's Input Back-Off.

Additionally, due to constellation warping and satellite channel induced ISI, the demodulator performance is degraded by an amount D (in dB) with respect to an ideal linear AWGN channel [De Gaudenzi *et al.*, 2006b]. This quantity D depends on the HPA distortion and hence on the IBO/OBO satellite characteristics (see e.g., Fig. 1). With this degradation, the effective SNR at the demodulator input $E_b/N_0|_{\text{eff}}$ is given by (in dB)

$$\left.\frac{E_b}{N_0}\right|_{sat}(IBO)=\left.\frac{E_b}{N_0}\right|_{eff}+OBO(IBO)+D(IBO) \tag{6}$$

Eq. (6) allows us to calculate an optimum HPA operating point which minimizes $E_b/N_0|_{\text{sat}}$. This point represents the best trade-off between the increasing power loss (OBO) related to the higher IBO and the reduction of the distortion (D) due to the improved linearity experienced by a larger IBO.

3. APSK constellation design optimization

3.1 Constellation description

M-APSK constellations are composed of n_R concentric rings, each with uniformly spaced PSK points. The signal constellation points x are complex numbers, drawn from a set $\mathfrak{X}$

$$\mathfrak{X}=\begin{cases} r_1\exp\left[j\left((2\pi/n_1)i+\theta_1\right)\right] & i=0,\ldots,n_1-1 \quad (Ring\ \ell=1) \\ r_2\exp\left[j\left((2\pi/n_2)i+\theta_2\right)\right] & i=0,\ldots,n_2-1 \quad (Ring\ \ell=2) \\ \vdots & \vdots \qquad\qquad \vdots \\ r_{n_R}\exp\left[j\left((2\pi/n_R)i+\theta_{n_R}\right)\right] & i=0,\ldots,n_{n_R}-1 \quad (Ring\ \ell=n_R) \end{cases} \tag{7}$$

where n_ℓ, r_ℓ and θ_ℓ $(\ell=1,\ldots,n_R)$ are defined as the number of points, the radius and the relative phase shift for the ℓ-th ring, respectively. Such modulation schemes are termed hereinafter as $n_1+n_2+\ldots+n_{n_R}-APSK$. Fig. 2 depicts the 4+12-APSK, 4+12+16-APSK and 4+12+16+32-APSK constellations. As mentioned above, for next generation standardized digital video broadcasting satellite systems, the constellation sizes of interest are $|\mathfrak{X}|=16$ and $|\mathfrak{X}|=32$ with n_R=2 and n_R=3 rings, respectively [DVB-S2, 2005; DVB-SH, 2007; GMR-1 3G, 2008; IPoS, 2006; Yuhai Shi *et al.*, 2008]. In addition, there has been an increasing commercial interest to go well beyond the standardized 16- and 32-APSK modes especially in professional DSNG applications where the constellation size of interest is $|\mathfrak{X}|=64$ with n_R=4 rings. In general, we consider that $\mathfrak{X}$ is normalized in energy, i.e., $E[|x|^2]=1$ which further implies that the radii r_ℓ are normalized such that $\sum_{\ell=1}^{n_R} n_\ell r_\ell^2=1$. Note also that the radii r_ℓ are ordered such that $r_1<r_2<\ldots<r_{n_R}$.

Furthermore, in order to reduce the dimensionality of the optimization problem, instead of optimizing the phase shifts θ_ℓ and the ring radii r_ℓ in absolute terms, the objective here is their optimization in relative terms. That is, we are looking for the optimum values of the phase shift of the ℓ-th ring with respect to the inner ring, $\phi_\ell=\theta_\ell-\theta_1$ $(\ell=1,\ldots,n_R)$, and of the relative radius of the ℓ-th ring with respect to the inner ring, $\rho_\ell=r_\ell/r_1$ $(\ell=1,\ldots,n_R)$, which satisfy a design optimization criterion. In particular, ϕ_1 =0 and ρ_1 =1. Thus, we are interested in finding an M-APSK constellation defined by the parameters $\boldsymbol{\rho}=(\rho_1,\rho_2,\ldots,\rho_{nR})$ and $\boldsymbol{\varphi}=(\varphi_1,\varphi_2,\ldots,\varphi_{nR})$ such that a given cost function $f(\mathfrak{X})$ reaches a maximum. As discussed next, the cost function employed here is the mutual information of the AWGN channel [De Gaudenzi *et al.*, 2006a; De Gaudenzi *et al.*, 2006b; Liolis & Alagha, 2008] which, unlike the more classical optimization criterion of the minimum Euclidean distance referring to the high SNR asymptotic case, provides an optimum M-APSK constellation $\mathfrak{X}$ for each coding

rate and modulation format Quasi-Error Free (QEF) SNR operating point or, equivalently, for each spectral efficiency R. We particularly assume a linear AWGN channel whereas robustness against nonlinear distortion is achieved in a subsequent step through exploitation of constellation pre-compensation (see Section 4).

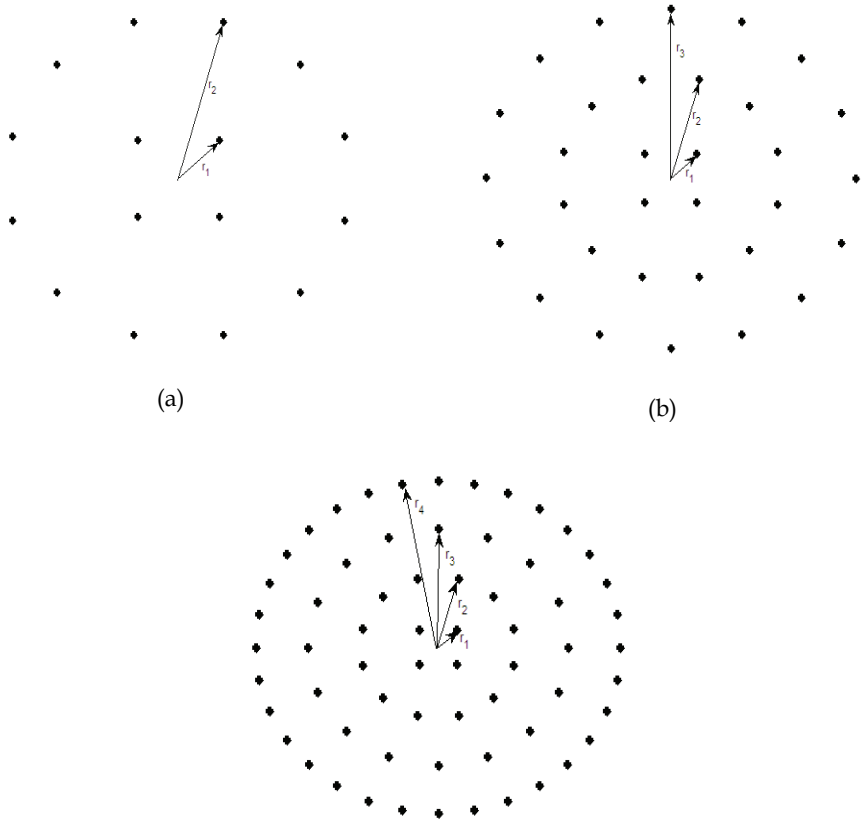

Fig. 2. M-APSK Constellations: (a) 16-APSK (4+12-APSK), (b) 32-APSK (4+12+16-APSK), (c) 64-APSK (4+12+16+32-APSK). The radii r_ℓ $(\ell = 1,...,n_R)$ of the multiple rings are also shown.

Next, two separate cases of APSK constellations are specifically examined with respect to the probability distribution of the constellation points $x \in \mathfrak{X}$:

- Equiprobable constellation points, that is, all constellation points $x \in \mathfrak{X}$ are equiprobable with probability $1/M$;
- Non-equiprobable constellation points, that is, the constellation points on each ℓ -th ring are assumed to be equiprobable but the *a priori* probability P_ℓ associated per ring is assumed different for each ring such that $\sum_{\ell=1}^{n_R} n_\ell P_\ell = 1$.

3.2 Equiprobable constellation optimization

In this case, all constellation points $x \in \mathfrak{X}$ are equiprobable with probability $1/M$, as considered in all standardized APSK modes so far [DVB-S2, 2005; DVB-SH, 2007; GMR-1 3G, 2008; IPoS, 2006; Yuhai Shi *et al.*, 2008]. The mutual information for a given APSK signal set $\mathfrak{X}$ provides the maximum transmission rate (in bits/channel use) at which error-free transmission is possible with such signal set and is given by [Ungerboeck, 1982]

$$f_{eq}\left(\mathfrak{X}\right) = I_{eq}\left(X;Y\right) = \log_2 M - \frac{1}{M}\sum_{k=0}^{M-1} E_w\left\{\log_2 \sum_{i=0}^{M-1} \exp\left[-\frac{E_s}{N_0}\left(\left|x^k + w - x^i\right|^2 - \left|w\right|^2\right)\right]\right\} \tag{8}$$

Thus, the optimization problem to be solved is formulated as

$$C_{eq}^{*} = \max_{\boldsymbol{\rho},\boldsymbol{\varphi}} f_{eq}\left(\mathfrak{X}\right) \tag{9}$$

In (8), $E\{\}$ denotes the expectation operator. We have particularly used expectation over the normally distributed noise variable w which is complex with variance N_0, i.e., $w \sim N_{\mathbb{C}}\left(0, N_0\right)$. In general, obtaining a closed-form expression for C^*_{eq} in (9) is a daunting task and so the Gauss-Hermite quadrature rules are employed for its numerical computation [Abramowitz & Stegun, 1964]. Numerical calculations of (9) for 16-, 32- and 64-APSK constellations are provided next in Sections 3.2.1-3.2.3.

However, for the asymptotic case $E_s/N_0 \to \infty$, it is possible to obtain a closed-form expression as follows. First, note that the expectation in (8) can be rewritten as

$$\lambda\left(\mathfrak{X}\right) \triangleq \frac{1}{M}\sum_{k=0}^{M-1} E_w\left\{\log_2 \sum_{i=0}^{M-1} \exp\left[-\frac{E_s}{N_0}\left(\left|x^k - x^i\right|^2 + 2\,\mathrm{Re}\left(\left(x^k - x^i\right)w\right)\right)\right]\right\} \tag{10}$$

Using the *Dominated Convergence Theorem* and the analysis presented in [De Gaudenzi *et al.*, 2006a], the influence of the noise term w vanishes asymptotically, since the limit can be pushed inside the expectation. Furthermore, the only remaining terms in the summation over $x^i \in \mathfrak{X}$ are $x^i = x^k$ and those closest in Euclidean distance $\delta^2_{\min} = \min_{x^i \in \mathfrak{X}} \left|x^i - x^k\right|^2$ which are in total $n_{min}(x^k)$. Therefore, taking the above into account as well as the approximation $\log_2\left(1+x\right) \simeq x \log_2 e$ for $|x| << 1$, $\lambda\left(\mathfrak{X}\right)$ in (10) comes up in the high SNR asymptotic case

$$\begin{aligned}\lambda\left(\mathfrak{X}\right) &\simeq \frac{1}{M}\sum_{k=0}^{M-1}\left\{\log_2\left[1 + n_{\min}\left(x^k\right)\exp\left(-\frac{E_s}{N_0}\delta^2_{\min}\right)\right]\right\} \simeq \frac{1}{M}\sum_{k=0}^{M-1}\left\{n_{\min}\left(x^k\right)\exp\left(-\frac{E_s}{N_0}\delta^2_{\min}\right)\log_2 e\right\} \\ &= \varepsilon \exp\left(-\frac{E_s}{N_0}\delta^2_{\min}\right)\end{aligned} \tag{11}$$

where ε is a constant which does not depend neither on the constellation minimum distance δ_{min} nor on SNR. Thus, after substituting (11) in (8), (9) yields

$$C^{*}_{eq}\Big|_{SNR\to\infty} = \max_{\boldsymbol{\rho},\boldsymbol{\varphi}}\left\{\log_2 M - \varepsilon \exp\left(-\frac{E_s}{N_0}\delta^2_{\min}\right)\right\} = \max_{\boldsymbol{\rho},\boldsymbol{\varphi}} \delta^2_{\min} \tag{12}$$

Eq.(12) clearly indicates that the maximization of the mutual information of the AWGN channel corresponds to the maximization of the minimum Euclidean distance in the asymptotic case of high SNR.

3.2.1 Numerical results for 16-APSK

Fig. 3 shows the numerical evaluation of (8) for a given range of values of $\rho_2 = r_2/r_1 = r_2$ and $\phi_2 = \theta_2 - \theta_1 = \theta_2$ for the 4+12-APSK constellation at E_s/N_0=12 dB. Surprisingly, there is no sensible dependence on φ. Therefore, the two-dimensional optimization can be achieved by simply finding the ρ_2 that maximizes AWGN channel capacity. This result is found to hold true also for the other constellations and hence, in the following, capacity optimization results do not account for relative phase shifts φ. Fig. 4 shows the union bound on the Symbol Error Probability (SER) for several 16-APSK modulations and for the optimum value of ρ_2 at R=3 bps/channel use (calculated as described above). Continuous lines indicate φ=0 while dotted lines refer to the maximum value of the relative phase shift, i.e. $\varphi=\pi/n_2$, showing no dependence on φ at high SNR. This absence of dependence on φ is justified by the fact that the optimum constellation separates the rings by a distance larger than the number of points in the ring itself, so that the relative phase φ has no significant impact in the distance spectrum of the constellation.

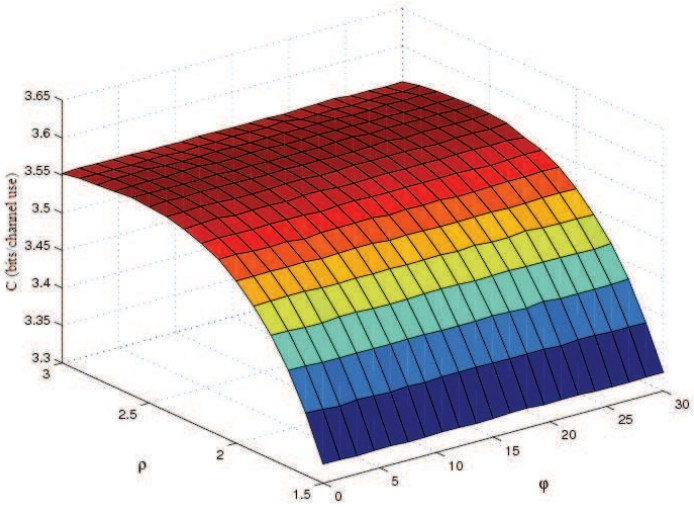

Fig. 3. Capacity surface for the 16-APSK (4+12) constellation at E_s/N_0=12 dB.

For 16-APSK it is also interesting to investigate the capacity dependency on n_1 and n_2. Fig. 5 depicts the modulation constrained capacity curves for several configurations of optimized 16-APSK constellations and compared with classical 16-QAM and 16-PSK signal sets. As can be observed, capacity curves are very close to each other, showing a slight advantage of 6+10-APSK over the rest. However, as discussed in [De Gaudenzi *et al.*, 2006b] and also in Section 4 below, 6+10-APSK and 1+5+10-APSK show other disadvantages compared to 4+12-APSK for phase recovery and nonlinear channel behaviour. All APSK optimized constellations are doing equal or better than 16QAM and significantly better than 16PSK.

Note also that there is a small gain, of about 0.2 dB, in using the optimized constellation for every spectral efficiency R rather than the one calculated with the minimum Euclidean distance (referring to high SNR asymptotic case).

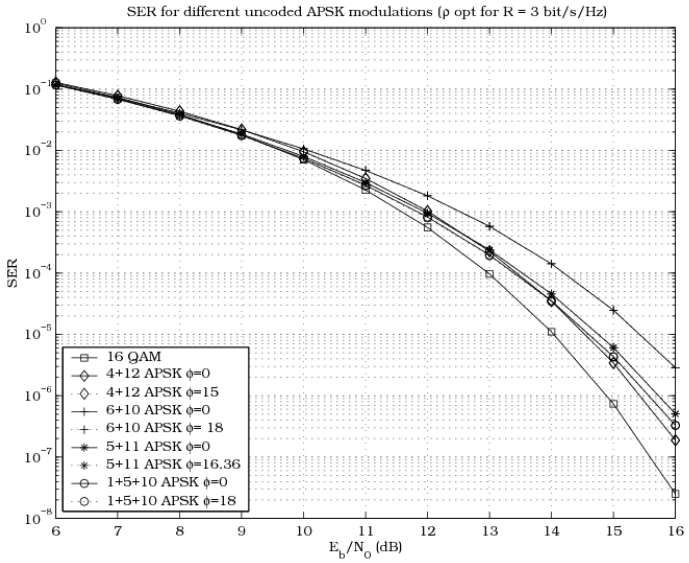

Fig. 4. Union bound on the uncoded SER for several 16-APSK modulations.

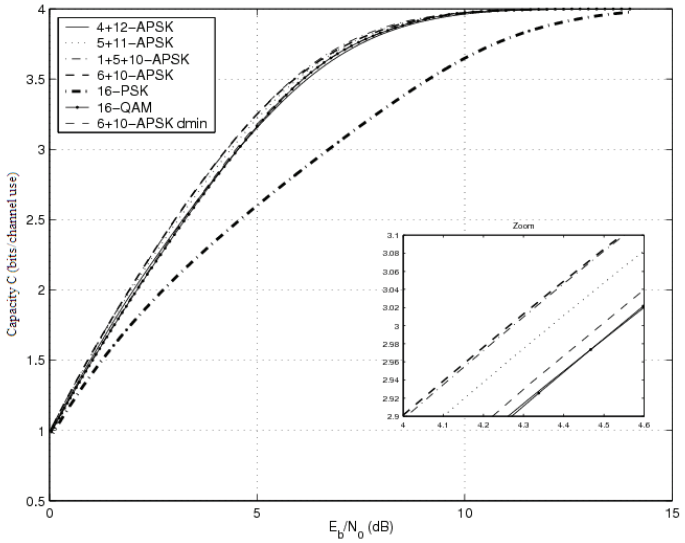

Fig. 5. Capacity of optimized 16-APSK constellations vs. 16-QAM and 16-PSK.

Table 1 below provides the optimized 16-APSK parameters for various coding rates r giving an optimum constellation for each given spectral efficiency R.

Modulation Order	Coding Rate r	Spectral Efficiency R (bps/Hz)	ρ_2^{opt}
4+12-APSK	2/3	2.67	3.15
4+12-APSK	3/4	3.00	2.85
4+12-APSK	4/5	3.20	2.75
4+12-APSK	5/6	3.33	2.70
4+12-APSK	8/9	3.56	2.60
4+12-APSK	9/10	3.60	2.57

Table 1. Optimized parameters for equiprobable 16-APSK constellation.

3.2.2 Numerical results for 32-APSK

Similarly, Fig. 6 presents the modulation constrained capacity of optimized 4+12+16-APSK (with the corresponding optimal values of ρ_2, ρ_3) compared to 32-QAM and 32-PSK. Again we observe slight capacity gain of 32-APSK over 32-QAM constellations for moderate to low SNR. The 32-APSK performance advantage versus 32-PSK is much more evident. Other 32-APSK constellations with different distribution of points in the three rings did not provide significantly better results.

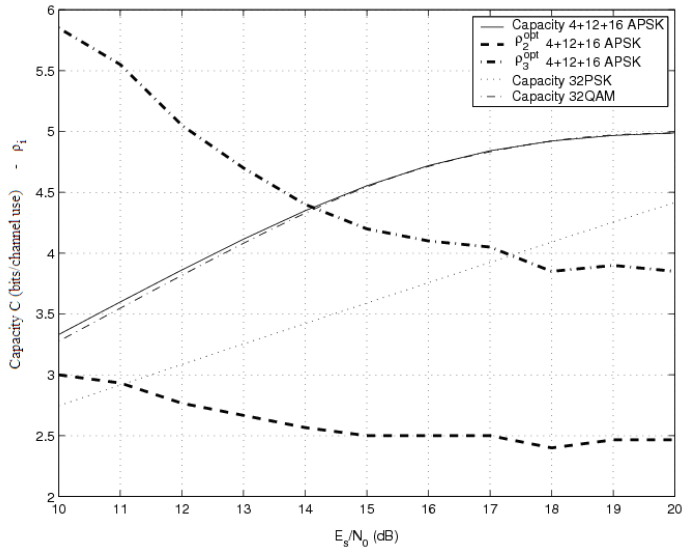

Fig. 6. Capacity and ρ^{opt} for the optimized 32-APSK constellations vs. 32-QAM and 32-PSK.

Table 2 below provides the optimized 32-APSK parameters for various coding rates r giving an optimum constellation for each given spectral efficiency R.

Note that the optimization results for 16- and 32-APSK reported in Tables 1 and 2 above have been adopted by the commercial standards related to satellite digital video broadcasting [DVB-S2, 2005; DVB-SH, 2007; GMR-1 3G, 2008; IPoS, 2006; Yuhai Shi *et al.*, 2008].

Modulation Order	Coding Rate r	Spectral Efficiency R (bps/Hz)	ρ_2^{opt}	ρ_3^{opt}
4+12+16-APSK	3/4	3.75	2.84	5.27
4+12+16-APSK	4/5	4.00	2.72	4.87
4+12+16-APSK	5/6	4.17	2.64	4.64
4+12+16-APSK	8/9	4.44	2.54	4.33
4+12+16-APSK	9/10	4.50	2.53	4.30

Table 2. Optimized parameters for equiprobable 32-APSK constellation.

3.2.3 Numerical results for 64-APSK

Fig. 7 presents the modulation constrained capacity along with the Shannon capacity bound versus the operating SNR for the 4+12+20+28-APSK constellation. In this case, the SNR range corresponds to coding rates r from 0.7 to 0.9. As can be observed, the penalty with respect to the Shannon limit ranges between 0.5 and 1.5 dB within the SNR range of interest. In the same figure, depicted is also the capacity penalty due to the suboptimal 4+12+20+28-APSK signal constellation setting if the minimum Euclidean distance maximization results (ρ_2=2.73, ρ_3=4.52 and ρ_4=6.31 [Benedetto *et al.*, 2005]) are instead taken into account. These results refer to the high SNR asymptotic case and so they are not optimized over the whole SNR range for each given spectral efficiency R. The latter statement is also illustrated in Fig. 7 where the optimal results in terms of mutual information maximization approach converge to the ones optimized based on minimum Euclidean distance maximization approach at high SNR values. It can also be observed that there is a small gain (of about 0.25 dB at SNR corresponding to coding rate r=0.7 which gets even less as the SNR - or r or R - increases) in using the optimized constellation for every R, rather than the calculated one with the minimum Euclidean distance criterion. Moreover, it can be seen that the relatively large penalty with respect to the Shannon limit within the SNR range of interest still remains in this case, as well.

Based on the findings in the case of 4+12+20+28-APSK above, there is no significant capacity gain in using the optimized constellation for each spectral efficiency R rather than the calculated one with the minimum Euclidean distance (or high SNR) criterion. Therefore, for the 4+12+16+32-APSK case, we have simply tested the previous optimization approach at high SNR and considered the (slightly) suboptimal results obtained over the whole SNR range for each coding rate r or spectral efficiency R. Following this approach, the resulting capacity achieved along with the Shannon capacity bound is plotted versus the operating SNR in Fig. 8. The SNR range depicted corresponds to coding rates r from 0.7 to 0.9. As can be seen, the penalty with respect to the Shannon limit ranges between 0.75 and 1.5 dB within the SNR range of interest.

From Fig. 7 and Fig. 8, it can be observed that there is no significant difference between the capacities of 4+12+20+28-APSK and 4+12+16+32-APSK constellations. Therefore, the preference of one constellation over the other has to be based on other performance criteria such as the signal Peak-to-Average Power Ratio (PAPR), synchronization issues, impact on nonlinearity, etc [De Gaudenzi *et al.*, 2006b].

Table 3 provides the optimized parameters taken into account in Fig. 7 and Fig. 8 for the cases of 4+12+20+28-APSK and 4+12+16+32-APSK constellations, respectively, for each

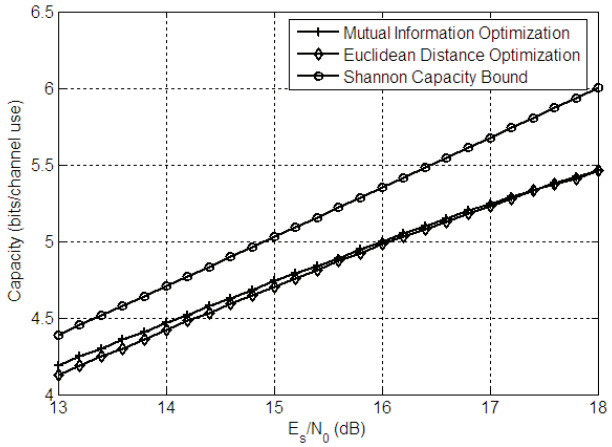

Fig. 7. Capacity of 64-APSK (4+12+20+28) constellation obtained through mutual information maximization and minimum Euclidean distance maximization approaches. Comparison with Shannon capacity bound.

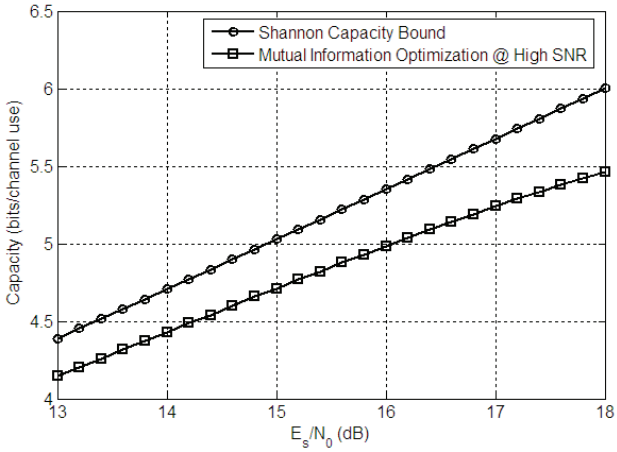

Fig. 8. Capacity of 64-APSK (4+12+16+32) constellation based on suboptimal parameters obtained for high SNR (minimum Euclidean distance maximization) and comparison with Shannon capacity bound.

given spectral efficiency R. The coding rates reported refer to the ones specified in the CCSDS Orange Book [CCSDS, 2007] which correspond to the ACM formats 25, 26, 27. As can be seen, only the optimized values of the relative radius of the ℓ -th ring with respect to the inner ring, $\rho_\ell^{opt}\left(\ell=2,3,4\right)$ are of rather importance and, therefore, reported. This is because there is no noticeable dependence on the relative phase shift φ as is the case also for 16- and 32-APSK. Particularly, in the case of 4+12+16+32-APSK, the (slightly) suboptimal parameters obtained for constellation design at high SNR are provided.

Modulation Order	Coding Rate r	Spectral Efficiency R (bps/Hz)	ρ_2^{opt}	ρ_3^{opt}	ρ_4^{opt}
4+12+20+28-APSK	0.798	4.79	2.62	4.58	7.00
4+12+20+28-APSK	0.841	5.05	2.58	4.40	6.56
4+12+20+28-APSK	0.896	5.38	2.50	4.14	6.00
4+12+16+32-APSK	-	-	2.60	4.20	6.00

Table 3. Optimized parameters for equiprobable 64-APSK constellation.

3.3 Non-Equiprobable constellation optimization

In the case of non-equiprobable constellation points, which has not been considered so far in any of the APSK related standards [DVB-S2, 2005; DVB-SH, 2007; GMR-1 3G, 2008; IPoS, 2006; Yuhai Shi *et al.*, 2008], shaping of *M*-APSK constellations is examined here in order to achieve the so called "shaping gain" [Calderbank & Ozarow, 1990; Forney & Wei, 1989]. To this end, assuming equiprobable constellation points on each ℓ-th ring which allows different *a priori* probabilities on different rings, a new APSK constellation design optimization problem is formulated and numerically solved in order to calculate the *a priori* probabilities of constellation points on each ℓ-th ring and also to calculate the corresponding shaping gain. The possible achieved shaping gain allows the reduction of the relatively large penalty with respect to the Shannon limit experienced with equiprobable constellation points (as shown in Section 3.2.3). The main idea behind constellation shaping is that signals with large norm are used less frequently than signals with small norm, thus improving the overall gain by adding shaping gain to the original coding gain. Theoretically, when constellation points are selected according to a continuous Gaussian distribution at every dimension, the maximum achievable shaping gain in the limit for infinite transmission rates is 1.53 dB [Calderbank & Ozarow, 1990; Forney & Wei, 1989]. Practically, a smaller shaping gain can be achieved in finite constellations as is the case in *M*-APSK constellations. From the above, it follows that the shaping again achieved in *M*-APSK constellations increases with the cardinality of signal set *M* and so it is expected to be greater in the case of 64-APSK than in the cases of 16- and 32-APSK.

Considering that the constellation points on each ring are equiprobable but the *a priori* symbol probability P_ℓ associated per each ℓ-th ring is different so that $\sum_{\ell=1}^{n_R} n_\ell P_\ell = 1$, and fixing the values of the relative radius and phase shift of each ℓ-th ring with respect to the inner ring to the optimized ones found in the equiprobable case (see Section 3.2 and Tables 1-3), a new constellation design optimization problem is formulated, which allows the calculation of the shaping gain. The cost function in this case is given by [Ungerboeck, 1982]

$$f_{non-eq}(\mathfrak{X}) = I_{non-eq}(X;Y) = -\sum_{k=0}^{M-1} Q(k) E_w \left\{ \log_2 \left[\sum_{i=0}^{M-1} Q(i) \exp\left[-\frac{E_s}{N_0} \left(\left| x^k + w - x^i \right|^2 - |w|^2 \right) \right] \right] \right\} \quad (13)$$

where $Q(k)$ denotes the *a priori* probability associated with each point $x^k \in \mathfrak{X}$. Equivalently,

$$Q(k)=\begin{cases} P_1 & k=0,1,\ldots,n_1-1 & (Ring\ \ell=1) \\ P_2 & k=n_1,n_1+1,\ldots,n_1+n_2-1 & (Ring\ \ell=2) \\ P_3 & k=n_1+n_2,n_1+n_2+1,\ldots,n_1+n_2+n_3-1 & (Ring\ \ell=3) \\ P_4 & k=n_1+n_2+n_3,n_1+n_2+n_3+1,\ldots,n_1+n_2+n_3+n_4-1 & (Ring\ \ell=4) \\ \vdots & \vdots & \vdots \\ P_{n_R} & k=M-n_R,M-n_R+1,\ldots,M-1 & (Ring\ \ell=n_R) \end{cases} \quad (14)$$

Thus, optimization over probability distribution is pursued in this case and the respective optimization problem to be solved is formulated as

$$C^*_{non-eq}=\max_{P_1,P_2,\ldots,P_{n_R}} f_{non-eq}(\mathfrak{X}) \quad (15)$$

where (as opposed to the equiprobable case addressed in Section 3.2) the parameters **ρ**, **φ** are now assumed fixed and the parameters to be optimized are the *a priori* probabilities $P_\ell\ (\ell=1,\ldots,n_R)$ which satisfy the condition $\sum_{\ell=1}^{n_R} n_\ell P_\ell=1$. Note that, since the probabilities P_ℓ are now varying, the signal set $\mathfrak{X}$ needs to be normalized in energy accordingly so that unit power is maintained [Calderbank & Ozarow, 1990]. $C^*_{non\text{-}eq}$ in (15) is numerically computed using the Gauss-Hermite quadrature rules [Abramowitz & Stegun, 1964]. Numerical calculations of (15) for 16-, 32- and 64-APSK constellations are provided next in Sections 3.3.1-3.3.3.

It is worth noting that in this new optimization problem, the number of the (free) optimization parameters is equal to the number of the *a priori* probabilities $P_\ell\ (\ell=1,\ldots,n_R)$ whereas the rest parameters of normalized ring radii $\rho_\ell=r_\ell/r_1$ are constrained (and fixed) to their optimum values obtained in Section 3.2. That is, the formulated optimization problem does not consider the optimum solution where all key optimization parameters (P_ℓ and ρ_ℓ) are considered free (in that case, the complexity of the optimization problem would significantly increase). However, it provides a good approximation to the near optimum solution for the *a priori* probabilities P_ℓ taking into account prior work on the optimization of the normalized ring radii ρ_ℓ. It also provides a rapid and efficient way to calculate the shaping gain achieved in each APSK mode as an upper bound on the potential spectral efficiency improvement. Note though that issues such as a possible increase in the transmit signal PAPR may limit the feasibility of achieving such gain.

3.3.1 Numerical results for 16-APSK

Following the optimization approach described above for the non-equiprobable 4+12-APSK constellation (its equiprobable 4+12-APSK counterpart refers to the standardized 16-APSK mode [DVB-S2, 2005; DVB-SH, 2007; GMR-1 3G, 2008; IPoS, 2006; Yuhai Shi *et al.*, 2008]), we obtain the near-optimal *a priori* probabilities P_1, P_2 for SNR operating points corresponding to coding rates r in the range of 2/3 to 9/10. The optimized constellation settings **ρ**, **φ** previously found in the equiprobable case and reported in Table 1 have been considered fixed. These optimization results are reported in Table 4 and illustrated in Fig. 9, as well. For the sake of comparison, the Shannon capacity bound and the capacity results for the equiprobable case have been plotted, as well. As can be seen, the constellation shaping

decreases the penalty with respect to the Shannon capacity bound. Namely, for spectral efficiency R=3 bits/channel use, the penalty with respect to the Shannon limit decreases from 0.9 dB (equiprobable case) to 0.6 dB (non-equiprobable case), whereas for R=3.5 bits/channel use, it decreases respectively from 1.5 dB to 1.2 dB. Therefore, the shaping gain for R=3 and 3.5 bits/channel use is about 0.3 dB in both cases.

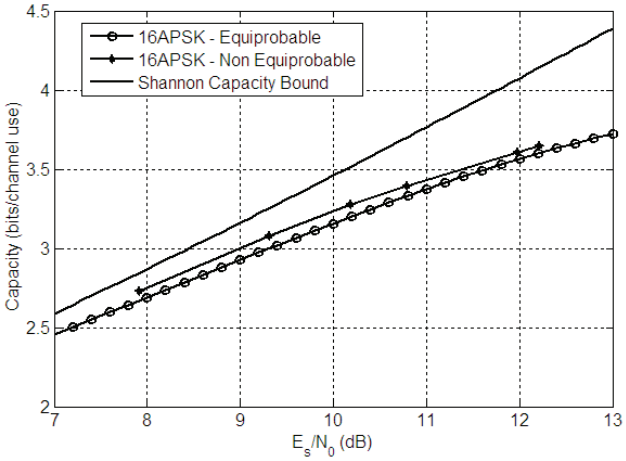

Fig. 9. Capacity and shaping gain of non-equiprobable 16-APSK (4+12) constellation.

Modulation Order	Coding Rate r	Spectral Efficiency R (bps/Hz)	P_1^{opt}	P_2^{opt}
4+12-APSK	2/3	2.73	0.116	0.045
4+12-APSK	3/4	3.08	0.115	0.045
4+12-APSK	4/5	3.27	0.109	0.047
4+12-APSK	5/6	3.40	0.105	0.048
4+12-APSK	8/9	3.61	0.095	0.052
4+12-APSK	9/10	3.64	0.093	0.052

Table 4. Optimized parameters for non-equiprobable 16-APSK constellation.

3.3.2 Numerical results for 32-APSK

Similarly, for the non-equiprobable 4+12+16-APSK constellation (its equiprobable 4+12+16-APSK counterpart refers to the standardized 32-APSK mode [DVB-S2, 2005; DVB-SH, 2007; GMR-1 3G, 2008; IPoS, 2006; Yuhai Shi *et al.*, 2008]), we obtain the near-optimal *a priori* probabilities P_1, P_2, P_3 for SNR operating points corresponding to coding rates r in the range of 3/4 to 9/10. The given optimized constellation settings $\boldsymbol{\rho}$, $\boldsymbol{\varphi}$ are fixed to those previously found in the equiprobable case and reported in Table 2. These optimization results are reported in Table 5 and illustrated in Fig. 10, as well. Similar results are achieved as in the case of non-equiprobable 4+12-APSK. As an illustration, the shaping gain for spectral efficiency R=4 and 4.5 bits/channel use is about 0.3 dB in both cases.

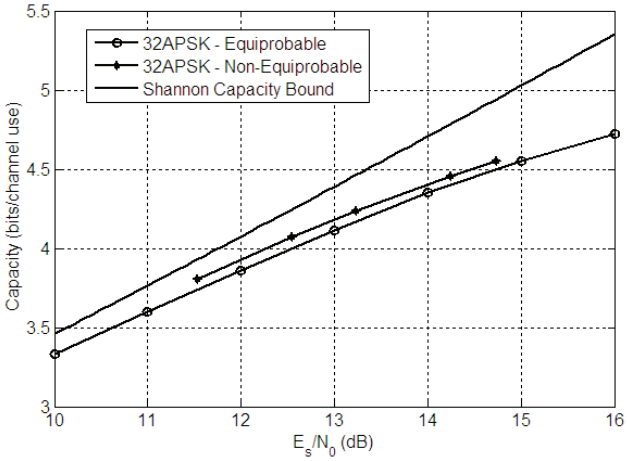

Fig. 10. Capacity and shaping gain of non-equiprobable 32-APSK (4+12+16) constellation.

Modulation Order	Coding Rate r	Spectral Efficiency R (bps/Hz)	P_1^{opt}	P_2^{opt}	P_3^{opt}
4+12+16-APSK	3/4	3.81	0.055	0.042	0.017
4+12+16-APSK	4/5	4.07	0.056	0.040	0.019
4+12+16-APSK	5/6	4.24	0.055	0.038	0.020
4+12+16-APSK	8/9	4.46	0.052	0.037	0.022
4+12+16-APSK	9/10	4.55	0.049	0.036	0.023

Table 5. Optimized constellation parameters for non-equiprobable 32-APSK.

3.3.3 Numerical results for 64-APSK

Similarly, for the non-equiprobable 4+12+20+28-APSK signal constellation set, we obtain the near optimal *a priori* probabilities P_1, P_2, P_3, P_4 for SNR operating points corresponding to coding rates r in the range of 0.82 to 0.91 for the given optimized constellation settings $\boldsymbol{\rho}$, $\boldsymbol{\varphi}$ previously found in the equiprobable case and reported in Table 3. These new optimization results are reported in Table 6 and illustrated in Fig. 11, as well. As can be seen, the constellation shaping decreases the penalty with respect to the Shannon capacity bound. Namely, for spectral efficiency R=5 bits/channel use, the penalty with respect to the Shannon limit decreases from 1 dB (equiprobable case) to 0.5 dB (non-equiprobable case), whereas for R=5.5 bits/channel use, it decreases respectively from 1.5 dB to 1.1 dB. Therefore, the shaping gain for R=5 and 5.5 bits/channel use is 0.5 dB and 0.4 dB, respectively.

Moreover, in the case of non-equiprobable 4+12+16+32-APSK signal constellation set, the near optimal *a priori* probabilities P_1,P_2,P_3,P_4 are obtained following a similar optimization approach whose results are presented in Table 7 and Fig. 12, as well. As an illustration in this case, the shaping gain achieved is 0.5 dB for spectral efficiency R=5 bits/channel use, whereas for R=5.5 bits/channel use, it is 0.3 dB.

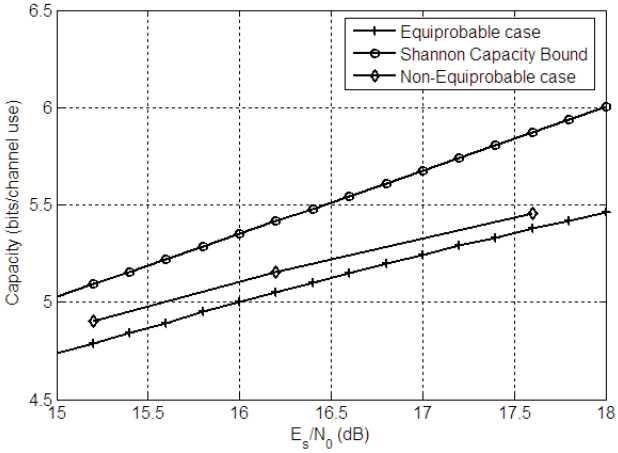

Fig. 11. Capacity and shaping gain of non-equiprobable 64-APSK (4+12+20+28) constellation.

Modulation Order	Coding Rate r	Spectral Efficiency R (bps/Hz)	P_1^{opt}	P_2^{opt}	P_3^{opt}	P_4^{opt}
4+12+20+28-APSK	0.817	4.90	0.040	0.025	0.020	0.0050
4+12+20+28-APSK	0.859	5.15	0.045	0.025	0.015	0.0079
4+12+20+28-APSK	0.910	5.46	0.040	0.025	0.015	0.0086

Table 6. Optimized constellation parameters for non-equiprobable 64-APSK (4+12+20+28).

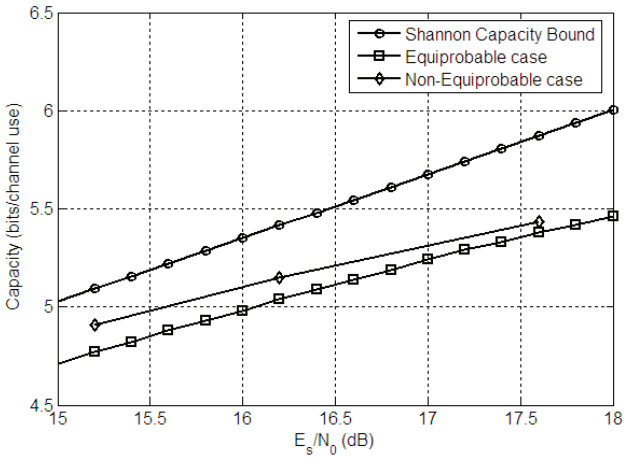

Fig. 12. Capacity and shaping gain of non-equiprobable 64-APSK (4+12+16+32) constellation.

Note that the present chapter does not go into further details on how to actually achieve the calculated shaping gain in the examined non-equiprobable 16-, 32- and 64-APSK modes; however, the interested readership might refer elsewhere in this regard, e.g., in [Calderbank & Ozarow, 1990; Forney & Wei, 1989].

Modulation Order	Coding Rate r	Spectral Efficiency R (bps/Hz)	P_1^{opt}	P_2^{opt}	P_3^{opt}	P_4^{opt}
4+12+16+32-APSK	0.818	4.91	0.051	0.028	0.019	0.0049
4+12+16+32-APSK	0.858	5.15	0.047	0.025	0.019	0.0065
4+12+16+32-APSK	0.905	5.43	0.040	0.022	0.018	0.0090

Table 7. Optimized constellation parameters for non-equiprobable 64-APSK (4+12+16+32).

4. Satellite channel distortion pre-compensation

Generally speaking, the HPA nonlinearity has two major effects. First, the varying constellation is distorted as the constellation points are mapped by the HPA nonlinear characteristic to a different point (amplitude, phase). Furthermore, the relative positions of the constellation points change. As briefly outlined above and discussed in detail next, this impairment can be efficiently reduced by ad-hoc pre-compensation at the transmitter. Despite its hardware complexity impact, commercial satellite modems have already adopted advanced dynamic pre-compensation techniques for standardized 16- and 32-APSK modes [Newtec, 2009]. Also, experimental laboratory measurement results for static pre-distortion techniques for standardized 16- and 32-APSK modes are reported in [Bischl *et al.*, 2009].

Second, ISI appears at the receiver as the HPA, although memoryless, is driven by a signal with controlled ISI due to the presence of the modulator SRRC filter. This leads to an overall nonlinear channel with memory. As a consequence, the demodulator SRRC is not matched anymore to the incoming signal. This issue is to be tackled mainly with a pre-equalization at the modulator [Karam & Sari, 1990] or equalization at the demodulator or a combination of the two techniques.

Although results presented in Section 3.2.1 indicated a slight superiority of 6+10-APSK, for nonlinear transmission over an amplifier, 4+12-APSK is preferable to 6+10-APSK because the presence of more points in the outer ring allows us to maximize the HPA DC power conversion efficiency. It is better to reduce the number of inner points, as they are transmitted at a lower power, which corresponds to a lower DC efficiency (the HPA power conversion efficiency is monotonic with the input power drive up to its saturation point). Fig. 13 shows the Probability Distribution Function (PDF) of the transmitted signal envelope for 16-QAM, 4+12-APSK, 6+10-APSK, 5+11-APSK, and 16-PSK; the shaping filter is an SRRC with roll-off factor a=0.35. As can be observed, the 4+12-APSK envelope is more concentrated around the outer ring amplitude than 16-QAM and 6+10-PSK, being remarkably close to the 16-PSK case. This shows that the selected constellation represents a good trade-off between 16-QAM and 16-PSK, with error performance close to 16-QAM, and

resilience to nonlinearity close to 16-PSK. Therefore, 4+12-APSK is preferable to the rest of 16-ary modulations considered. Similar advantages have been observed for 32-APSK compared to 32-QAM [De Gaudenzi *et al.*, 2006a].

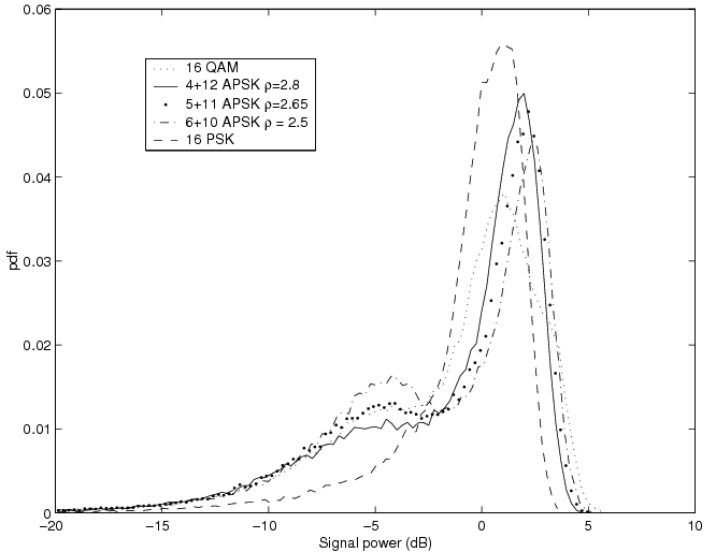

Fig. 13. Simulated histogram of the transmitted signal envelope power for 16-ary APSK, QAM and PSK constellations.

4.1 Static pre-compensation

The simplest approach for counteracting the HPA nonlinear characteristic is to modify the complex-valued constellation points at the modulator side. Thanks to the multiple-ring nature of the APSK constellation, pre-compensation is easily done by a simple modification of the parameters **ρ**, **φ**. The known AM/AM and AM/PM HPA characteristics (see, e.g., Fig.1) are exploited in order to obtain a good replica of the desired signal constellation geometry after the HPA, as if it had not suffered any distortion. This can be simply obtained by artificially increasing the relative radii ρ_ℓ and modifying the relative phases $\phi_\ell \left(\ell = 1,...,n_R \right)$ at the modulator side.

The calculation of the pre-distorted constellation parameters can be made with the technique described in [De Gaudenzi & Luise, 1995] for the computation of the distorted constellation center of mass (*centroids*) seen at the demodulator matched filter output. With knowledge of the satellite link characteristics, the static pre-compensation parameters can be calculated off-line by taking the following steps:

1. Generation of *S* blocks of *W* symbols over which the Symbol Matched Filter (SMF) centroids are computed (transmission in the absence of white noise);
2. Computation of the error signal at the end of each block;
3. Pre-distorted constellation point update.

The latter task can be readily achieved through an iterative Least Mean Square (LMS) type of algorithm illustrated by the following set of equations:

$$\begin{cases} \left|x_{pre}^{(n)}\right|(s+1) = \left|x_{pre}^{(n)}\right|(s) - \gamma_r \cdot e_c^{(n)}(s) \\ \arg\left(x_{pre}^{(n)}(s+1)\right) = \arg\left(x_{pre}^{(n)}(s)\right) - \gamma_\phi \cdot \psi(s) \\ e_c^{(n)}(s) = r_c^{(n)}(s) \cdot \exp\left(j\theta_c^{(n)}(s)\right) - \left|x^{(n)}\right| \\ r_c^{(n)}(s) \cdot \exp\left(j\theta_c^{(n)}(s)\right) = \dfrac{1}{W} \cdot \sum\limits_{k \in l^n, sW+1 \le k \le (s+1)W} y(k) \\ \psi(s) = \begin{cases} \arg\left(e_c^{(n)}(s)\right) - 2\pi & , \quad \arg\left(e_c^{(n)}(s)\right) > \pi \\ \arg\left(e_c^{(n)}(s)\right) + 2\pi & , \quad \arg\left(e_c^{(n)}(s)\right) < -\pi \\ \arg\left(e_c^{(n)}(s)\right) & , \quad \left|\arg\left(e_c^{(n)}(s)\right)\right| \le \pi \end{cases} \end{cases} \tag{16}$$

where the index n refers to the constellation point, $l^{(n)}$ indicates the conditioning to the constellation point n, s refers to the iteration step of the algorithm, $y(k)$ represents the k-th SMF output complex sample, $x^{(n)}$ represents the APSK complex constellation reference point, $r_c^{(n)}(s)$ and $\theta_c^{(n)}(s)$ are the modulus and the phase of the SMF output complex n-th centroid computed at step s, $x_{pre}^{(n)}(s)$ is the pre-distorted n-th constellation point computed at step s, γ_r and γ_φ the adaptation steps for the pre-distorted constellation point modulus and the phase, respectively.

As an illustration, based on Fig. 14(a), the optimal 4+12-APSK pre-distortion parameters are $\rho_2' = 3.5$ and $\Delta\varphi$=25 deg for an IBO=3 dB whereas $\rho_2' = 3.7$ and $\Delta\varphi$=27 deg for a smaller IBO=2 dB. As expected, the pre-distorted constellation is expanded, e.g., $\rho_2' > \rho_2$. For the new constellation points x', they are $x' \in \mathfrak{X}$ i.e., they still follow (7) but with new radii r'_i such that $F(r'_i) = r_i$ (i=1,2).

Concerning the phase, it is possible to pre-correct for the effect of the HPA on the phase HPA between inner and outer rings through a simple change in the relative phase shift by $\phi_2' = \phi_2 + \Delta\phi$, with $\Delta\phi = \phi(r_2') - \phi(r_1')$. These operations can be readily implemented in the digital modulator by simply modifying the reference constellation parameters $\boldsymbol{\rho}'$, $\boldsymbol{\varphi}'$ with *no hardware complexity impact* or out-of-band emission increase at the linear modulator output. However, it should be remarked that static pre-compensation may imply an increase of the transmitted signal PAPR, which in turn may have a potential impact of the out-of-band emissions after the HPA. The compensation effort is shifted into the modulator side, allowing the use of an optimal demodulator/decoder for AWGN channels even when the HPA is close to saturation. Based on (1), the signal at the modulator output is then

$$s_T^{pre} = \sqrt{P} \sum_{k=0}^{L-1} x'(k)\, p_T(t - kT_s) \tag{17}$$

where now $x'(k) \in \mathfrak{X}'$ being the pre-distorted symbols with ρ_ℓ', ϕ_ℓ' $(\ell = 1,\ldots,n_R)$.

To show the effect of this practical static pre-distortion technique, the scatter diagram at the output of the SRRC (with roll-off factor a=0.35) receiver matched filter is shown in Fig. 14(b) for 16-APSK with IBO=2 dB. For clarity, the scatter diagram at the SMF has been obtained in

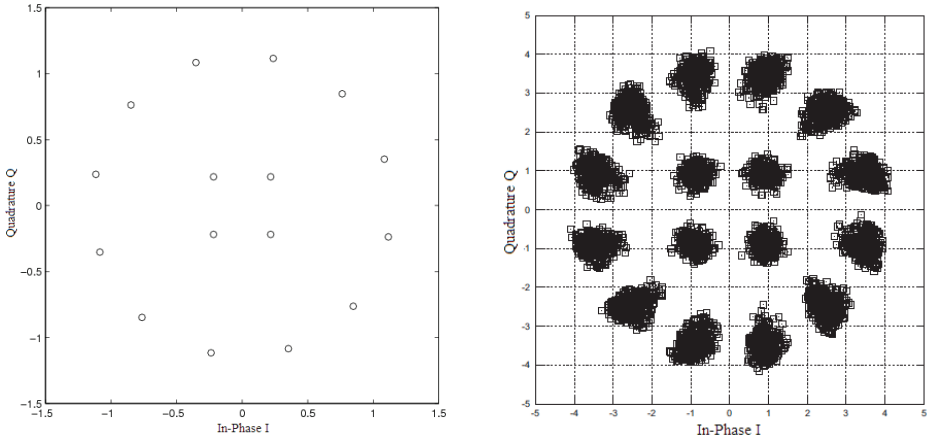

(a) (b)

Fig. 14. Static pre-compensation for 4+12-APSK constellation: (a) Modulator output roll-off factor a=0.35 with static pre-compensation (ρ_2=3.7 and $\Delta\varphi$=27 deg); (b) Demodulator SRRC filter output noiseless scatter diagram in the nonlinear channel for IBO=2 dB, roll-off factor a=0.35 with static pre-compensation (ρ_2=3.7 and $\Delta\varphi$=27 deg).

the absence of AWGN. Despite the strong channel nonlinearity, the center of mass corresponding to the scattered diagram closely follows the optimum 4+12-APSK constellation, for which the optimum parameters are ρ_2=2.7 and φ=0.

Measurements showed that the HPA characteristic sensitivity to temperature or aging results in a limited change of gain but not in a modification of the AM/AM, AM/PM characteristics shape. The limited gain variations are compensated by the satellite transponder Automatic Level Control (ALC) device, thus off-line pre-compensation has a long term value. If required, the compensated parameters can be adapted to track larger slow variations in HPA characteristic due to aging.

Further experimental laboratory measurement results for such static pre-distortion techniques for the standardized 16- and 32-APSK modes are reported in [Bischl *et al.*, 2009].

4.2 Dynamic pre-compensation

Static pre-distortion is able to compensate for the constellation warping effects but not for the clustering phenomenon. To this end, an extension of the static pre-distortion algorithm described above has been adopted and further improved in [Casini *et al.*, 2004]. The dynamic pre-distortion algorithm takes into account the memory of the channel, conditioning the pre-distorted modulator constellation not only to the current symbol transmitted but also to the *(L-1)/2* preceding and *(L-1)/2* following symbols (*L* being the number of symbols in total). This calls for an increased look-up table size of *ML* points. By exploiting the APSK constellation symmetry, the amount of memory size can be reduced to *3ML/16*.

The advantage provided by the dynamic pre-compensation on the reduction of the clustering effect can be assessed by observing the scatter diagram at the SMF sampler output shown in Fig. 15(b) and 15(c). Looking at Fig. 15(a), it appears that the clustering effect reduction is obtained at the expenses of an increased outer constellation points' amplitude. This corresponds to a peak to average signal envelope ratio of 10 dB compared to 6.77 dB in

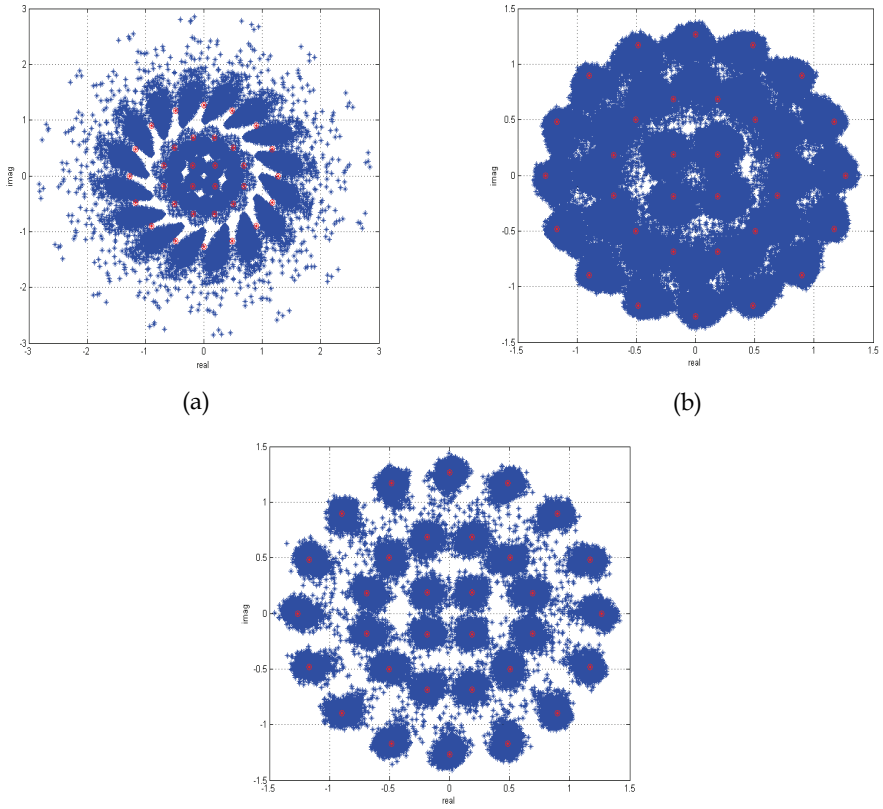

Fig. 15. Dynamic pre-distortion on 32APSK, with IBO=3.6 dB, W=5000 symbols, s=85 blocks, L=3: a) blue crosses pre-distorted constellation, red circles nominal constellation, b) blue crosses constellation centroids at the demodulator SMF, red circles nominal constellation without pre-compensation, c) blue crosses constellation centroids at the demodulator SMF, red circles nominal constellation with dynamic pre-compensation.

the case of static pre-compensation. The dynamic pre-distortion induced PAPR increase has two main drawbacks: a) the augmentation of the HPA OBO which negatively affects the overall system efficiency, b) the possible impact on the HPA TWTA safe operation due to the higher PAPR making the instantaneous signal power occasionally well beyond the saturation point. Based on these considerations, an improved dynamic pre-distortion approach has been devised. The quantity to minimize is in fact not the Root Mean Squared (RMS) of the centroids conditioned to a certain data pattern but rather the total link degradation D_{TOT} (in dB) given by [Casini *et al.*, 2004]

$$D_{TOT}(s) = \frac{E_s}{N_0}\bigg|_{req}^{NL}(\mathrm{s}) - \frac{E_s}{N_0}\bigg|_{req}^{AWGN}(\mathrm{s}) + OBO(s) \tag{18}$$

where $\left(E_s/N_0\right)\Big|_{req}^{NL}$ and $\left(E_s/N_0\right)\Big|_{req}^{AWGN}$ are the average symbol energy over noise density required to achieve the target Frame Error Rate (FER) in the nonlinear and linear AWGN channel, respectively. By using the Gaussian approximation for the ISI at the SMF sampler output one can write:

$$\left[\frac{E_s}{N_0}\right]_{req}^{NL}(s)=\left[\frac{E_s}{N_0}\right]_{req}^{AWGN}(s)\left[1+\frac{\sigma_{ISI}^2(s)}{N_0}\right] \tag{19}$$

where $\sigma^2_{ISI}(s)$ represents the ISI power at the output of the SMF averaged over the constellation points at step s, that is, in mathematical terms

$$\sigma_{ISI}^2(s)=\frac{1}{M}\sum_{n=1}^{M}\sum_{k\in l^{(n)},\ sW+1\le k\le(s+1)W}\left\{z(k)-c^{(n)}\right\}^2 \tag{20}$$

By replacing (19) into (18) we get

$$D_{TOT}(s)=\left[1+\frac{\sigma_{ISI}^2(s)}{N_0}\right]OBO(s) \tag{21}$$

Eq. (21) is valid in the case of absence of intra-system co-channel and adjacent channel interference. These two quantities, in fact, depend on the signal energy so that an increase of the OBO does not affect the signal-to-interference ratio. It is easy to show that, if I_0^{SAT} denotes the total power of the intra-system interference samples at the SMF output with OBO=0 dB, (21) can be generalized as

$$D_{TOT}(s)=\left[1+\frac{\sigma_{ISI}^2(s)+\dfrac{I_0^{SAT}}{OBO(s)}}{N_0}\right]OBO(s) \tag{22}$$

Since I_0^{SAT} is system-dependent, next we assume a situation where intra-system interference is negligible, so that its contribution does not affect the pre-distortion optimization results.
The dynamic pre-compensation is now performed as described before computing every block of W symbols also the σ^2_{ISI} and OBO and computing (21) at each step. The dynamic pre-compensation is now stopped when the minimum of D_{TOT} is achieved. This approach ensures the best trade-off between ISI minimization and the OBO penalty due to the increased PAPR caused by dynamic pre-compensation. To speed-up process convergence and to avoid bias in the σ^2_{ISI} estimate, the static pre-compensation is first applied then the dynamic pre-compensation is started. This approach allows beginning the dynamic pre-compensation with the SMF centroids very close to the nominal constellation points. An example of the D_{TOT} -based optimized dynamic pre-compensation is illustrated in Fig. 16. In this figure the D_{TOT} and OBO evolution versus the iteration number s is plotted for the case of 8PSK. It appears that after the minimum of D_{TOT} occurring around s=30 blocks, after this value the total loss is growing following the OBO growth due to the transmit constellation outer points expansion.

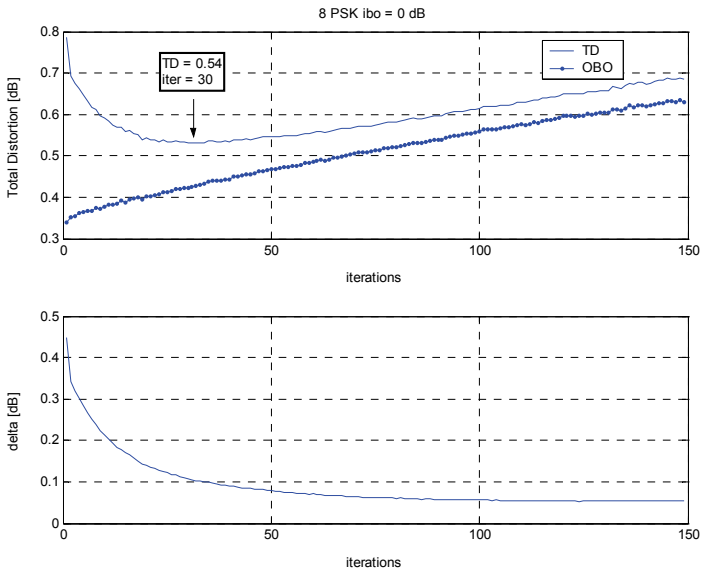

Fig. 16. D_{TOT} and *OBO* evolution vs. time with dynamic pre-distortion on 8PSK, with IBO = 0 dB, W=50000 symbols.

Performance improvements for dynamic pre-distortion are quite remarkable for high order constellations. As reported in [Casini *et al.*, 2004], in case of 16-APSK, the advantage for exploiting dynamic pre-compensation amounts to about 0.8 dB compared to static pre-compensation while the dynamic optimization brings about 0.2 dB improvement. In case of 32-APSK, the advantage for exploiting dynamic pre-compensation amounts to about 1.8 dB compared to static pre-compensation and about 3.5 dB compared to non pre-distorted constellations.
It is also worth noting that commercial satellite modems have already adopted similar advanced dynamic pre-compensation techniques [Newtec, 2009].

5. Conclusions

This chapter has presented analysis and numerical results on the design of APSK signal constellation sets which are well suited for advanced satellite digital video broadcasting systems. The APSK constellation modes examined are the 16-, 32- and 64-ary whereas the design optimization criterion employed has been the maximization of the AWGN channel mutual information. The presented analysis has taken into account both equiprobable and non-equiprobable APSK constellations where a respective optimization problem has been formulated and numerically solved. In addition, practical static and dynamic pre-distortion techniques for pre-compensation of the satellite channel nonlinearities have been addressed.
In particular, the design optimization technique based on the mutual information maximization has been shown to extend the more traditional one based on the minimum Euclidean distance maximization, yielding a small but significant improvement, especially for the 16- and 32-APSK modes. Following this optimization approach, the optimal

constellation settings, more specifically, the optimum normalized radii of the APSK constellation rings, have been determined as a function of the operating SNR. Optimization results have indicated no significant dependency on the relative phase shifts between the multiple rings of APSK constellation in all cases of 16-, 32- and 64-ary modes at the target SNR operating points. The presented results for 16- and 32-APSK equiprobable constellations have already been adopted by commercial standards related to satellite digital video broadcasting.

In the case of non-equiprobable 16-, 32- and 64-APSK signal sets, constellation shaping has been examined, the near optimal *a priori* probabilities associated with each ring have been evaluated and the respective shaping gain has been calculated reaching values of up to 0.5 dB for the target SNR operating regions.

In addition, the impact of typical satellite channel nonlinearities as well as techniques to counteract their impact on the demodulator performance have been analyzed. It has been shown that coded APSK with simple digital pre-distortion techniques based on look-up tables can achieve very good performance with satellite HPA driven at saturation (16-APSK) or with limited back-off (32-APSK). Special emphasis has been put on practical dynamic pre-distortion techniques which achieve remarkable performance improvements for 16-and 32-APSK constellations and which have recently been adopted in commercial satellite modems for the relevant nonlinear channel pre-compensation.

6. References

[Abramowitz & Stegun, 1964] Abramowitz M., and Stegun I.A. (eds.), *Handbook of Mathematical Functions*, Appl. Math. Ser. No. 55, National Bureau of Standards, Washington, D.C., 1964.

[Alberty *et al.*, 2007] Alberty E., Defever S., Moreau C., De Gaudenzi R., Ginesi A., Rinaldo R., Gallinaro G., and Vernucci A, "Adaptive Coding and Modulation for the DVB-S2 Standard Interactive Applications: Capacity Assessment and Key System Issues", *IEEE Wireless Communications*, vol. 14, no. 4, pp. 61-69, August 2007.

[Benedetto *et al.*, 2005] Benedetto S., Garello R., Montorsi G., Berrou C., Douillard C., Giancristofaro D., Ginesi A., Giugno L., and Luise M., "MHOMS: High-Speed ACM Modem for Satellite Applications", *IEEE Wireless Communications Magazine*, vol. 12, no. 2, pp. 66-77, April 2005.

[Bischl *et al.*, 2009] Bischl H., Brandt H., De Cola T., De Gaudenzi R., Eberlein E., Girault N., Alberty E., Lipp S., Rinaldo R., Rislow B., Arthur Skard J., Tousch J., and Ulbricht J., "Adaptive coding and modulation for satellite broadband networks: From theory to practice", to appear in *International Journal on Satellite Communications and Networking*, DOI: 10.1002/sat.932, 2009.

[Calderbank & Ozarow, 1990] Calderbank A.R., and Ozarow L.H., "Nonequiprobable signalling on the Gaussian channel", *IEEE Transactions on Information Theory*, vol.36, no.4, pp.726-740, July 1990.

[Casini *et al.*, 2004] Casini E., De Gaudenzi R., and Ginesi A., "DVB-S2 modem algorithms design and performance over typical satellite channels", *International Journal on Satellite Communications and Networking*, vol. 22, no. 3, pp. 281-318, May/June 2004.

[CCSDS, 2007] Flexible Serially Concatenated Convolutional Turbo Codes with Near-Shannon Bound Performance for Telemetry Applications, *CCSDS Orange Book*, Issue 1, September 2007, CCSDS 131.2-O-1.

[De Gaudenzi & Luise, 1995] De Gaudenzi R., and Luise M., "Design and analysis of an all-digital demodulator for trellis coded 16-QAM transmission over a nonlinear satellite channel," *IEEE Transactions on Communications*, vol. 43, no. 2/3/4-Part I, February/March/April, 1995.

[De Gaudenzi *et al.*, 2006a] De Gaudenzi R., Guillén i Fàbregas A. & Martinez A., "Turbo-coded APSK modulations design for satellite broadband communications", *International Journal of Satellite Communications and Networking*, vol. 24, pp. 261-281, 2006.

[De Gaudenzi *et al.*, 2006b] De Gaudenzi R., Guillén i Fàbregas A. & Martinez A., "Performance analysis of turbo-coded APSK modulations over nonlinear satellite channels", *IEEE Transactions on Wireless Communications*, vol.5, no.9, pp. 2396-2407, September 2006.

[DVB-S2, 2005] ETSI EN 302 307 V1.1.1 (2005-03), Digital Video Broadcasting (DVB); "Second generation framing structure, channel coding and modulation systems for broadcasting interactive services, news Gathering and other broadband satellite applications".

[DVB-SH, 2007] ETSI EN 302 583 V1.1.1 (2007-07), Digital Video Broadcasting (DVB); "Framing structure, channel coding and modulation for Satellite services to Handheld devices (SH) below 3 GHz".

[Forney & Wei, 1989] Forney G.D., and Wei L.F., "Multidimensional constellations – Part I: Introduction, figures of merit, and generalized cross constellations", *IEEE Journal on Selected Areas in Communications*, vol.7, no.6, pp.877-892, August 1989.

[Future Internet, 2009] Future Internet: The Cross-ETP (European Technology Platform) Future Internet Strategic Research Agenda, Version 1.0, July 2009 [Available on-line at EU Future Internet portal: www.future-internet.eu].

[GMR-1 3G, 2008] ETSI TS 101 376-5-4 V2.3.1 (2008-08), GMR-1 3G, "GEO-Mobile Radio Interface Specifications (Release 2); General Packet Radio Service; Part 5: Radio interface physical layer specifications; GMPRS-1".

[Hughes, 2009] Hughes Network Systems (HNS) IP over Satellite Technology [Available on-line at: www.hughes.com].

[IPoS, 2006] ETSI TS 102 354 V1.2.1 (2006-11), Satellite Earth Stations and Systems (SES); Broadband Satellite Multimedia (BSM); Transparent Satellite Star - B (TSS-B); "IP over Satellite (IPoS) Air Interface Specification".

[Karam & Sari, 1990] Karam G., and Sari H., "Data predistortion techniques using intersymbol interpolation," *IEEE Transactions on Communications*, vol. 38, no. 10, pp. 1716–1723, October 1990.

[Karam & Sari, 1991] Karam G., and Sari H., "A Data Predistortion Technique with Memory for QAM Radio Systems," *IEEE Transactions on Communications*, vol. 39, no. 2, pp 336–44, February 1991.

[Liolis & Alagha, 2008] Liolis K.P., and Alagha N.S., "On 64-APSK Constellation Design Optimization", in Proc. *10th International Workshop on Signal Processing for Space Communications* (SPSC'08), Rhodes, Greece, October 2008.

[Newtec, 2009] Newtec EL470 IP Satellite Modem [Available on-line at: www.newtec.eu].

[Rinaldo & De Gaudenzi, 2004a] Rinaldo R., and De Gaudenzi R., "Capacity analysis and system optimization for the forward link of multi-beam satellite broadband

systems exploiting adaptive coding and modulation", *International Journal on Satellite Communications and Networking*, vol. 22, no. 3, pp. 401-423, May/June 2004.

[Rinaldo & De Gaudenzi, 2004b] Rinaldo R., and De Gaudenzi R., "Capacity analysis and system optimization for the reverse link of multi-beam satellite broadband systems exploiting adaptive coding and modulation", *International Journal on Satellite Communications and Networking*, vol. 22, no. 4, pp. 425-448, July/August 2004.

[Sung *et al.*, 2009] Sung W., Kang S., Kim P., Chang D.-I., and Shin D.-J., "Performance analysis of APSK modulation for DVB-S2 transmission over nonlinear channels", *International Journal on Satellite Communications and Networking*, vol. 27, 2009.

[Thomas *et al.*, 1974] Thomas C.M., Weidner M.Y., and Durrani S.H., "Digital amplitude phase keying with M-ary alphabets," *IEEE Transactions on Communications*, vol. 22, no. 2, pp. 168–180, February 1974.

[Ungerboeck, 1982] Ungerboeck G., "Channel coding with multilevel phase signals", *IEEE Transactions on Information Theory* , vol.28, no.1, pp. 55–67, 1982.

[Yuhai Shi *et al.*, 2008] Yuhai Shi, Ming Yang, Ju Ma, and Rui Lv, "A New Generation Satellite Broadcasting System in China: Advanced Broadcasting System-Satellite", in Proc. 4*th* *International Conference on Wireless Communications, Networking and Mobile Computing* (WiCOM'08), Dalian, China, October 2008.

Digital Video

Edited by Floriano De Rango

ISBN 978-953-7619-70-1
Hard cover, 500 pages
Publisher InTech
Published online 01, February, 2010
Published in print edition February, 2010

This book tries to address different aspects and issues related to video and multimedia distribution over the heterogeneous environment considering broadband satellite networks and general wireless systems where wireless communications and conditions can pose serious problems to the efficient and reliable delivery of content. Specific chapters of the book relate to different research topics covering the architectural aspects of the most famous DVB standard (DVB-T, DVB-S/S2, DVB-H etc.), the protocol aspects and the transmission techniques making use of MIMO, hierarchical modulation and lossy compression. In addition, research issues related to the application layer and to the content semantic, organization and research on the web have also been addressed in order to give a complete view of the problems. The network technologies used in the book are mainly broadband wireless and satellite networks. The book can be read by intermediate students, researchers, engineers or people with some knowledge or specialization in network topics.

InTech Europe
University Campus STeP Ri
Slavka Krautzeka 83/A
51000 Rijeka, Croatia
Phone: +385 (51) 770 447
Fax: +385 (51) 686 166
www.intechopen.com

InTech China
Unit 405, Office Block, Hotel Equatorial Shanghai
No.65, Yan An Road (West), Shanghai, 200040, China
中国上海市延安西路65号上海国际贵都大饭店办公楼405单元
Phone: +86-21-62489820
Fax: +86-21-62489821